DEVELOPMENT AND ANALYSIS OF A MATHEMATICAL MODEL OF CARBON POLLUTION LEVEL ON KENYAN HIGHWAYS WITH HUGE EMBANKMENTS

John Otieno Awino
Department of Mathematics and Computer Science,
The Catholic University Of Eastern Africa, Kenya

Thomas Onyango
Department of Industrial and Engineering Mathematics,
The Technical University of Kenya

N. B. Okelo
Department of Pure and Applied Mathematics,
Jaramogi Oginga Odinga University of Science and Technology, Kenya

Abstract

Carbon pollution on highways is attributed to major health problems experienced by those who stay along the highways. Most existing models developed by researchers have shown that CO which is the cause of many diseases suffered by those who stay close to highways. However, most researches have shown lack of mechanistic understanding of how roadside barriers affect pollutant transport and transformation on and near roadways, especially under different meteorological conditions and barrier properties, for example highway embankment. In this study we have therefore constructed a mathematical model incorporating embankment as a parameter. The black carbon concentration in the atmosphere along highways at different time scales will be simulated numerically using Finite Volume Method (FVM), with assumption that presence of embankment affects the physical parameters such as convection, Advection and diffusion.

INTRODUCTION

Highway vehicles release billions of tons of gases into the atmosphere per year. The major component of these gases is black carbon which is produced from the vehicles exhaust due to incomplete combustion of the diesel. Diesel exhaust is a source of atmospheric soot and fine particles which constitute a fraction of air pollution implicated in human diseases such as cancer, heart and lung related diseases, the concentration of soot along the highways is more if the highways are embanked [19].

MATHEMATICAL MODELS OF AIR POLLUTION

Governing Equation

This study has used a numerical solution of the three-dimensional steady state diffusion equation for a finite width line source that was adopted by Goyal and Anikender in [25] as a numerical methodology to solve Boundary Layer Model for Air Pollutant Concentrations Due to Highway Traffic with several modifications.

$$\frac{\partial C}{\partial t} + u\frac{\partial C}{\partial x} + v\frac{\partial C}{\partial y} + w\frac{\partial C}{\partial z} = \frac{\partial}{\partial x}\left(K_x\frac{\partial C}{\partial x}\right) + \frac{\partial}{\partial y}\left(K_y\frac{\partial C}{\partial y}\right) + \frac{\partial}{\partial z}\left(K_z\frac{\partial C}{\partial z}\right) + S \quad \text{..... (1)}$$

Where c= (ρ-ρ0) with the x-axis oriented along the wind vector, u, the y-axis cross-wind and the z-axis oriented vertically upward, and where u= u (z)is the wind speed in the x-direction,

C= C(x, y, z) is the ambient concentration of the carbon pollutant species, $v = v_y\ (z)$ is the turbulent eddy diffusivity in the cross-wind direction,$w = w_z(z)$ is the turbulent eddy diffusivity in the vertical direction. Considering steady state condition $(i.e\frac{\partial C}{\partial t} = 0)$,with the vertical velocity component neglected and x-oriented in the direction of the mean wind (i.e. u=U, v=O),where K_x, K_y and K_z are eddy diffusivities along the x, y, and z directions. They further considered the following assumptions

- unsteady state condition $(i.e\frac{\partial C}{\partial t} \neq 0)$
- the vertical velocity component (W) is neglected
- x-axis is oriented in the direction of mean wind (i.e. u=U, v=0)
- downwind diffusion is neglected in comparison to transport due to mean wind.
- density of pure air is a constant ρ_0

The model reduced to

$$\frac{\partial C}{\partial t} + u\frac{\partial C}{\partial x} = \frac{\partial}{\partial y}\left(K_y\frac{\partial C}{\partial y}\right) + \frac{\partial}{\partial z}\left(K_z\frac{\partial C}{\partial z}\right) + S \quad \text{.....(2)}$$

INITIAL AND BOUNDARY CONDITIONS

The boundary conditions used are Dirichlet and Neumann B.C. which are natural B.Cs

Dirichlet boundary condition (total absorption)

$$\left.\begin{matrix} C(x,y=0 \\ C(x,y) = h \end{matrix}\right\} \quad \text{.....(3)}$$

Neumann boundary (total reflection)

$$\left.\begin{matrix} K_y\frac{\partial C(x,y)}{\partial y} = 0, \text{at y} = 0 \\ K_y\frac{\partial C(x,y)}{\partial y} = 0, \text{at y} = \text{h} \end{matrix}\right\} \quad \text{..... (4)}$$

Mixed (type-I) boundary condition

$$\left.\begin{matrix} K_y\frac{\partial C(x,y)}{\partial y} = 0, \text{at y} = 0 \\ \text{C(x,y)} = \ 0, \text{at y} = \text{h} \end{matrix}\right\} \quad \text{..... (5)}$$

Where C= $(\rho-\rho_0)$ per unit volume,ρ_0 is the density of pure air, ρ is the density of polluted air.

Adiabatic boundary condition at x=0 and x=H for $t \geq 0$

$$\left.\begin{aligned} \frac{\partial C(x,y)}{\partial x} &= 0, \text{ at } x = 0 \\ K_x \frac{\partial C(x,y)}{\partial x} &= 0, \text{ at } x = H \end{aligned}\right\} \quad \ldots\ldots\ldots\ldots\ldots\ldots (6)$$

$C = \rho - \rho_0$ C=0 implies that $\rho = \rho_0$ at all the boundaries

The vector of conserved variables and fluxes for the two- dimensional conservation law for the hydrodynamics are worked out as follows:

Recall the hydrodynamics equations, 18, 19, and 20 stated below

$$\frac{\partial \rho}{\partial t} + \nabla.(\rho\vec{V}) = S_\rho + S_D$$

$$\frac{\partial(\rho\vec{V})}{\partial t} + [(\rho\vec{V}.\nabla)\vec{V}] = -\nabla P + \rho g + S_V, \text{ and}$$

$$\frac{\partial E}{\partial t} + \nabla.(E\vec{V}) = -\nabla.(P\vec{V}) + S_E$$

$$U_t = \frac{dU}{dt} = \frac{d\rho}{dt} \rightarrow \quad U = \rho$$

In the x-direction

$$\frac{dU}{dt} = \frac{d(\rho u)}{dt} \quad \rightarrow \quad U = \rho u$$

In the y-direction

$$\frac{dU}{dt} = \frac{d(\rho v)}{dt} \quad \rightarrow \quad U = \rho v$$

$$\nabla.\rho u = F(U)_x \quad \rightarrow \quad U = E$$

Therefore in vector form U is given as

$$U = \begin{bmatrix} \rho \\ \rho u \\ \rho v \\ E \end{bmatrix}$$

In the x-direction

$$\nabla.(\rho u^2 + P) = F(U)_x \quad \rightarrow \quad F = \rho u^2 + P$$

In the y-direction

$\nabla.(\rho uv) = F(U)_X \rightarrow F = \rho uv$

Also, $\nabla.(Eu + uP) = F(U)_x \rightarrow F = u(E + P)$

Therefore in vector form F is given by

$$F = \begin{bmatrix} \rho u \\ \rho u^2 \\ \rho uv \\ u(E+P) \end{bmatrix}$$

$$U = \begin{bmatrix} \rho \\ \rho u \\ \rho v \\ E \end{bmatrix}, F = \begin{bmatrix} \rho u \\ \rho u^2 \\ \rho uv \\ u(E+P) \end{bmatrix} \quad \text{..... (26)}$$

APPROXIMATE CONSERVATION LAWS

Consider the one dimensional conservation law

$U_t + F(U)_x = 0$

If the Jacobian matrix $A(U) = \frac{\partial F}{\partial U}$ is used, the conservation law can be written as

$U_t + A(U)U_x = 0$ ..... (27)

The method of Roe approximates equation (23) by replacing the Jacobian matrix by a constant Jacobian matrix

$\tilde{A} = \tilde{A}(U_L, U_R)$

where U_L and U_R are the left and right solutions to the original PDE. So we replace the original PDE of a linear system with constant coefficients of the form

$U_t + \tilde{A}U_x = 0$ .....(28)

We further substitute the original Riemann problem by approximate Riemann problem that we can be able to solve exactly with the same initial conditions. If we generally let the hyperbolic system consist of m conservation laws, then Roe's Jacobian matrix $\tilde{A}$ is the one required to satisfy the following properties; To ensure the approximate problem presenting mathematical character of the original non-linear system, hyperbolicity of the system requires that $\tilde{A}$ will consist of m real eigenvalues associated with the corresponding flux term, the flux,F in the one-dimensional case that depends on the left and right hand solution of the original PDE, $\lambda_i^{(F)} = \lambda_i^{(F)}(U_L, U_R)$. The order is chosen to be $\lambda_1^{(F)} \leq \lambda_2^{(F)} \leq --- \leq \lambda_m^{(F)}$ along with

eigenvectors associated with the flux F. To ensure consistency with the conservation laws, it is required that the system has consistency with the exact Jacobian. $\tilde{A}(U,U) = A(U)$

To ensure conservation, it is required that the system has conservation across discontinuities $F(U_R) - F(U_L) = \tilde{A}(U_R - U_L)$ ……..…….(29)

APPROXIMATE CONSERVATION LAWS FOR ISOTHERMAL EULER EQUATIONS

We assume an isothermal system through time, to simplify the algebraic expressions and derivations. In this case sound speed a, is given by $a = \sqrt{\frac{\partial P}{\partial \rho}}$, and thus the pressure is given by

$P = a^2\rho.$ ……...(30)

Isothermal systems are idealistic and are common assumptions. Maintaining a system at a constant temperature requires a heat flux through the boundaries to manage the generated or lost by the system. In real life system, the temperature of a gas will never remain exactly constant; however, it may relax towards a constant temperature very quickly as energy flows in or out of the gas. In any case, isothermal systems still give an important insight into the physical interpretation of the system. Consider the sourceless conservation of mass and Navier-Stokes equations

$$\frac{\partial \rho}{\partial t} + \nabla.(\rho\vec{V}) = 0$$

$$\frac{\partial(P\vec{V})}{\partial t} + \left[(\rho\vec{V}.\nabla)\vec{V}\right] = -\nabla P + \rho g$$

Which we write in matrix form as

$$\begin{bmatrix}\rho\\ \rho u\\ \rho v\end{bmatrix}_t + \begin{bmatrix}\rho u\\ P+\rho u^2\\ \rho uv\end{bmatrix}_x + \begin{bmatrix}\rho v\\ \rho uv\\ P+\rho V^2\end{bmatrix}_y = 0 \quad \ldots\ldots\ldots\ldots (31)$$

We can write the Euler equations, equation (31) in conservation law form as

$U_t + F(U)_x + G(U)_y = 0$ ……..…… (32)

Now we introduce Jacobian matrix, $A(U) = \frac{\partial F}{\partial U}$and $B(U) = \frac{\partial G}{\partial U}$, equation [32] becomes

$U_t + A(U)U_x + B(U)U_y = 0$

Roe's approach replaces the Jacobian matrix by a constant Jacobian matrix.

$\tilde{A} = \tilde{A}(U_L, U_R)\tilde{B} = \tilde{B}(U_L, U_R)$

The original system is therefore replaced by linear approximate of Riemann problem

$$U_t + A(U)U_x + B(U)U_y = 0$$

$$U(x,y,0) = \begin{cases} U_L x, y < 0 \\ U_R x, y > 0 \end{cases}$$

In this case the numerical flux's F and G can be solved for independently, along the associated eigenvalues and eigenvectors. Therefore we must have system of conservation law equations

$$\left.\begin{aligned} U_t + \tilde{A}U_x = 0 \\ U_t + \tilde{B}U_y = 0 \end{aligned}\right\} \quad \text{..... (33)}$$

4.3 THE NUMERICAL FLUX

From Equation 33, we need to solve each conservation law independent from the other. This method is called the approximate Riemann problem. Consider the equation using the flux F,

$U_t + F(U)_x = 0$Where the isothermal Euler equation gives

$$U = \begin{bmatrix} \rho \\ \rho u \\ \rho v \end{bmatrix}, \qquad F = \begin{bmatrix} \rho u \\ a + \rho u^2 \\ \rho uv \end{bmatrix} = \begin{bmatrix} F_1 \\ F_2 \\ F_3 \end{bmatrix}$$

The Jacobi matrix hence becomes

$$\tilde{A} = \frac{\partial F}{\partial U} = \begin{bmatrix} \frac{\partial F_1}{\partial(\rho)} & \frac{\partial F_1}{\partial(\rho u)} & \frac{\partial F_1}{\partial(\rho v)} \\ \frac{\partial F_2}{\partial(\rho)} & \frac{\partial F_2}{\partial(\rho u)} & \frac{\partial F_2}{\partial(\rho v)} \\ \frac{\partial F_3}{\partial(\rho)} & \frac{\partial F_3}{\partial(\rho u)} & \frac{\partial F_3}{\partial(\rho v)} \end{bmatrix} \quad \text{.....(34)}$$

In order to perform the partial differentiation, the flux components must be determined in terms of the variables for which the partial derivative is being taken with respect to.

FIRST ROW

The first component $\frac{\partial F_1}{\partial(\rho)} = \frac{\partial(\rho u)}{\partial(\rho)} = 0$

Second component, $\frac{\partial F_1}{\partial(\rho u)} = \frac{\partial(\rho u)}{\partial(\rho)} = 1$

And third component $\frac{\partial F_1}{\partial(\rho v)} = \frac{\partial(\rho u)}{\partial(\rho v)} = 0$

SECOND ROW

The first component, $\frac{\partial F_2}{\partial(\rho)} = \frac{\partial(a+\rho u^2)}{\partial(\rho)} = a^2 - u^2$

Second component, $\frac{\partial F_2}{\partial(\rho u)} = \frac{\partial(a+\rho u^2)}{\partial(\rho u)} = \frac{\partial(\rho u^2)}{\partial(\rho u)} = 2u$

And third component, $\frac{\partial F_2}{\partial(\rho v)} = \frac{\partial(a+\rho u^2)}{\partial(\rho v)} = 0$

THIRD ROW

The first component, $\frac{\partial F_3}{\partial(\rho)} = \frac{\partial(\rho uv)}{\partial(\rho)} = \frac{\partial}{\partial(\rho)}\left[\frac{(\rho u)(\rho v)}{\rho}\right] = -\frac{(\rho u)(\rho v)}{\rho^2} = -uv$

Second component, $\frac{\partial F_3}{\partial(\rho u)} = \frac{\partial(\rho uv)}{\partial(\rho u)} = \frac{\partial}{\partial(\rho u)}\left[\frac{(\rho u)(\rho v)}{\rho}\right] = v$

And the third component, $\frac{\partial F_3}{\partial(\rho v)} = \frac{\partial(\rho uv)}{\partial(\rho v)} = \frac{\partial}{\partial(\rho v)}\left[\frac{(\rho u)(\rho v)}{\rho}\right] = u$

Therefore, the Jacobi matrix for the F numerical flux is

$$\tilde{A} = \frac{\partial F}{\partial U} = \begin{bmatrix} 0 & 1 & 0 \\ a^2 - u^2 & 2u & 0 \\ -uv & v & u \end{bmatrix} \quad \text{..... (35)}$$

Now we consider the numerical flux G, for equation

$U_t + G(U)_y = 0$

$$U = \begin{bmatrix} \rho \\ \rho u \\ \rho v \end{bmatrix}, \qquad G = \begin{bmatrix} \rho v \\ \rho uv \\ a + \rho v^2 \end{bmatrix} = \begin{bmatrix} G_1 \\ G_2 \\ G_3 \end{bmatrix}$$

The Jacobian matrix is determined by

$$\tilde{B} = \frac{\partial G}{\partial U} = \begin{bmatrix} \frac{\partial G_1}{\partial(\rho)} & \frac{\partial G_1}{\partial(\rho u)} & \frac{\partial G_1}{\partial(\rho v)} \\ \frac{\partial G_2}{\partial(\rho)} & \frac{\partial G_2}{\partial(\rho u)} & \frac{\partial G_2}{\partial(\rho v)} \\ \frac{\partial G_3}{\partial(\rho)} & \frac{\partial G_3}{\partial(\rho u)} & \frac{\partial G_3}{\partial(\rho v)} \end{bmatrix} \text{.....(36)}$$

We now perform partial differentiation, to determine the flux components in terms of the variables for which the partial derivative is being taken with respect to.

FIRST ROW

The first component $\frac{\partial G_1}{\partial(\rho)} = \frac{\partial(\rho v)}{\partial(\rho)} = 0$

Second component, $\frac{\partial G_1}{\partial(\rho u)} = \frac{\partial(\rho v)}{\partial(\rho u)} = 0$

And third component $\frac{\partial F_1}{\partial(\rho v)} = \frac{\partial(\rho v)}{\partial(\rho v)} = 1$

SECOND ROW

The first component, $\frac{\partial G_2}{\partial(\rho)} = \frac{\partial(\rho uv)}{\partial(\rho)} = \frac{\partial}{\partial(\rho)}\left[\frac{(\rho u)(\rho v)}{\rho}\right] = -\frac{(\rho u)(\rho v)}{\rho^2} = -uv$

Second component, $\frac{\partial G_2}{\partial(\rho u)} = \frac{\partial(\rho uv)}{\partial(\rho u)} = \frac{\partial}{\partial(\rho u)}\left[\frac{(\rho u)(\rho v)}{\rho}\right] = v$

And the third component, $\frac{\partial G_2}{\partial(\rho v)} = \frac{\partial(\rho uv)}{\partial(\rho v)} = \frac{\partial}{\partial(\rho v)}\left[\frac{(\rho u)(\rho v)}{\rho}\right] = u$

THIRD ROW

The first component, $\frac{\partial G_3}{\partial(\rho)} = \frac{\partial(a+\rho v^2)}{\partial(\rho)} = a^2 - v^2$

Second component, $\frac{\partial G_3}{\partial(\rho u)} = \frac{\partial(a+\rho v^2)}{\partial(\rho u)} = 0$

And third component, $\frac{\partial G_3}{\partial(\rho v)} = \frac{\partial(a+\rho v^2)}{\partial(\rho v)} = \frac{\partial(\rho v^2)}{\partial(\rho v)} = 2v$

Therefore, the Jacobi matrix for the G numerical flux is

$$\tilde{B} = \frac{\partial G}{\partial U} = \begin{bmatrix} 0 & 0 & 1 \\ -uv & v & u \\ a^2 - v^2 & 0 & 2v \end{bmatrix} \quad \text{.....(37)}$$

We can now be able to determine the eigenvalues and corresponding eigenvectors now that numerical fluxes have been determined.

ROE MATRIX

At this point we now need to determine the eigenvalues and eigenvectors corresponding to each Jacobian matrix for each flux, F and G. Our solution is determined by averaging over the left and right solutions to the original system.

Equation (36) gives the Jacobian matrix for the numerical flux F.

$$\tilde{A} = \begin{bmatrix} 0 & 1 & 0 \\ a^2 - u^2 & 2u & 0 \\ -uv & v & u \end{bmatrix}$$

The eigenvalues of $\tilde{A}$ are found by solving eigenequation $|\tilde{A} - \lambda I| = 0$

Performing substitution in $\tilde{A}$ gives,

$$|\tilde{A} - \lambda I| = \begin{vmatrix} -\lambda & 1 & 0 \\ a^2 - u^2 & 2u - \lambda & 0 \\ -uv & v & u - \lambda \end{vmatrix}$$

$$= -\lambda\big((2u - \lambda)(u - \lambda)\big) - 1\big((a^2 - u^2)(u - \lambda)\big)$$

$$= (u - \lambda)[-\lambda(2u - \lambda) - (a^2 - u^2)]$$

Therefore, $(u - \lambda)[\lambda(2u - \lambda) - (a^2 - u^2)] = 0$

$$(u - \lambda)[\lambda^2 - 2\lambda u - (a^2 - u^2)] = 0$$

$$\lambda = u \text{and} [\lambda^2 - 2\lambda u - (a^2 - u^2)] = 0 \rightarrow \lambda = \frac{2u \pm \sqrt{4u^2 + 4(a^2 - u^2)}}{2} = u \pm a$$

The eigenvalues are therefore,

$$\lambda_1^{(F)} = u, \qquad \lambda_2^{(F)} = u + a, \qquad \lambda_3^{(F)} = u - a \quad \text{...} (38)$$

We now determine the right eigenvectors first. The first eigenvalue is $\lambda_1^{(F)} = u$

Therefore, $[\tilde{A} - \lambda I] . \begin{bmatrix} \tilde{K}_{R_1}^{(F)} \\ \tilde{K}_{R_2}^{(F)} \\ \tilde{K}_{R_3}^{(F)} \end{bmatrix} = 0$

Since we are considering the right-hand side, the u and v velocities are taken from right to left as well.

$$[\tilde{A} - \lambda_1^{(F)} I] . \begin{bmatrix} \tilde{K}_{R_1}^{(F)} \\ \tilde{K}_{R_2}^{(F)} \\ \tilde{K}_{R_3}^{(F)} \end{bmatrix} = \begin{bmatrix} -u_R & 1 & 0 \\ a^2 - u_R^2 & u_R & 0 \\ -u_R v_R & v_R & 0 \end{bmatrix} . \begin{bmatrix} \tilde{K}_{R_1}^{(F)} \\ \tilde{K}_{R_2}^{(F)} \\ \tilde{K}_{R_3}^{(F)} \end{bmatrix} = 0 \text{...} (39)$$

The corresponding system of equations is given by,

$$\begin{cases} 0 = -u_R \tilde{K}_{R_1}^{(F)} + \tilde{K}_{R_2}^{(F)} \\ 0 = (a^2 - u_R^2)\tilde{K}_{R_1}^{(F)} + u_R \tilde{K}_{R_2}^{(F)} \\ 0 = -u_R v_R \tilde{K}_{R_1}^{(F)} + v_R \tilde{K}_{R_2}^{(F)} \end{cases} \quad \text{.....(40)}$$

Given the determinant does not varnish, the trivial solution is obtained as,

$$\tilde{K}_{R_1}^{(F)} = \begin{bmatrix} 0 \\ 0 \\ 1 \end{bmatrix} \quad \text{.....(41)}$$

The second right eigenvector corresponds to the eigenvalue, $\lambda_2^{(F)} = u + a$ and hence the eigenequation becomes,

$\left[\tilde{A} - \lambda_2^{(F)} I\right].\begin{bmatrix} \tilde{K}_{R_1}^{(F)} \\ \tilde{K}_{R_2}^{(F)} \\ \tilde{K}_{R_3}^{(F)} \end{bmatrix} = 0$, and substitution yields,

$$\left[\tilde{A} - \lambda_2^{(F)} I\right].\begin{bmatrix} \tilde{K}_{R_1}^{(F)} \\ \tilde{K}_{R_2}^{(F)} \\ \tilde{K}_{R_3}^{(F)} \end{bmatrix} = \begin{bmatrix} -u_R - a & 1 & 0 \\ a^2 - u_R^2 & u_R - a & 0 \\ -u_R v_R & v_R & a \end{bmatrix}.\begin{bmatrix} \tilde{K}_{R_1}^{(F)} \\ \tilde{K}_{R_2}^{(F)} \\ \tilde{K}_{R_3}^{(F)} \end{bmatrix} = 0 \quad \text{.....(42)}$$

Therefore the eigenvector becomes,

$$\tilde{K}_{R_2}^{(F)} = \begin{bmatrix} 1 \\ u_R - a \\ v_R \end{bmatrix}$$

The final right eigenvector corresponds to eigenvalue, $\lambda_3^{(F)} = u - a$ and the eigenequation becomes,

$$\left[\tilde{A} - \lambda_3^{(F)} I\right].\begin{bmatrix} \tilde{K}_{R_1}^{(F)} \\ \tilde{K}_{R_2}^{(F)} \\ \tilde{K}_{R_3}^{(F)} \end{bmatrix} = 0 \quad \text{.....(43)}$$

Hence, $\left[\tilde{A} - \lambda_3^{(F)} I\right].\begin{bmatrix} \tilde{K}_{R_1}^{(F)} \\ \tilde{K}_{R_2}^{(F)} \\ \tilde{K}_{R_3}^{(F)} \end{bmatrix} = \begin{bmatrix} -u_R + a & 1 & 0 \\ a^2 - u_R^2 & u_R + a & 0 \\ -u_R v_R & v_R & a \end{bmatrix}.\begin{bmatrix} \tilde{K}_{R_1}^{(F)} \\ \tilde{K}_{R_2}^{(F)} \\ \tilde{K}_{R_3}^{(F)} \end{bmatrix} = 0$ .....(44)

The eigenvector is, $\tilde{K}_{R_3}^{(F)} = \begin{bmatrix} 1 \\ u_R + a \\ v_R \end{bmatrix}$

The columns of the right Roe matrix for the flux, F corresponds to the right eigenvector of the Jacobian matrix. Thus the right Roe matrix is

$$R_R^{(F)} = \left[\tilde{K}_{R_1}^{(F)}, \tilde{K}_{R_2}^{(F)}, \tilde{K}_{R_3}^{(F)},\right] = \begin{bmatrix} 1 & 0 & 1 \\ u_R - a & 0 & u_R + a \\ v_R & 1 & v_R \end{bmatrix}$$

We can thus deduce from the above right Roe matrix, the left Roe matrix. Hence,

$$R_L^{(F)} = \left[\tilde{K}_{L_1}^{(F)}, \tilde{K}_{L_2}^{(F)}, \tilde{K}_{L_3}^{(F)},\right] = \begin{bmatrix} 1 & 0 & 1 \\ u_L - a & 0 & u_L + a \\ v_L & 1 & v_L \end{bmatrix}$$

Therefore, the averaged Roe matrix corresponding to the Jacobian matrix F is given by

$$\tilde{R}^{(F)} = \left[\tilde{K}_1^{(F)}, \tilde{K}_2^{(F)}, \tilde{K}_3^{(F)},\right] = \begin{bmatrix} 1 & 0 & 1 \\ \tilde{u} - a & 0 & \tilde{u} + a \\ \tilde{v} & 1 & \tilde{v} \end{bmatrix} \quad \text{(45)}$$

The averaged Roe matrix corresponding to the Jacobian matrix for the flux G is given by

$$\tilde{R}^{(G)} = \left[\tilde{K}_1^{(G)}, \tilde{K}_2^{(G)}, \tilde{K}_3^{(G)},\right] = \begin{bmatrix} 1 & 0 & 1 \\ \tilde{u} & -1 & \tilde{u} \\ \tilde{v} - a & 0 & \tilde{v} + a \end{bmatrix} \quad \text{(46)}$$

SOUCE TERM FOR FINITE VOLUME METHOD

We need to implement the source term into the FVM. Now we add the source term to the original sourceless conservation law, Equation 32

$$U_t + F(U)_x + G(U)_y = 0$$

Adding the source term transforms it to

$$U_t + F(U)_x + G(U)_y = S(U)$$

In matrix form $\begin{bmatrix} \rho \\ \rho u \\ \rho v \end{bmatrix}_t + \begin{bmatrix} \rho u \\ a + \rho u^2 \\ \rho uv \end{bmatrix} + \begin{bmatrix} \rho v \\ \rho uv \\ a + \rho v^2 \end{bmatrix} = \begin{bmatrix} S_\rho + S_D \\ 0 \\ -\rho g + S_v \end{bmatrix}$

The source term takes the form

$$S_D = D\nabla^2 = D\nabla^2 = D\nabla.(\nabla\rho)$$

$$S_\rho = \begin{cases} f(y), & y \geq y_0 \\ 0, & y < y_0 \end{cases}$$

$$S_v = S_\rho V_{ey} \tilde{y}.$$

where $f(y) = S_{\rho 0} e^{\frac{-(y-y_0)}{x_0}}$ and $S_{\rho 0} = \frac{\rho_{e0} V_{ey}}{x_0}$

Given the pollutant parameters$\rho_{e0} = 0.1\rho_0$, $V_{ey} = 15\text{m/s}$, $\rho_0 = 1.290 kg/m^3$, is the density of pure air and diffusion coefficient $D = 0.2\, cm^2/s = 2 \times 10^{-5}\, m^2/s$

In order to solve this system we need a code. Therefore the results of the FVM will be presented in this chapter four along with a conclusion summarizing the research project.

LEVEL OF CARBON POLLUTION ON KENYAN HIGHWAYS

The level of emission of carbon from a road was given in [23] as 315635.17 tons per annum. The transport sectors in Kenya contribute 23% of the total carbon emission. Road transport currently accounts for 74% of total transport of carbon emission as reported in [26]. On global level, CO_2 emission grew by 51% between 1990 and 2012 [27].The Environmental Management Bureau showed that motor vehicles contribute about 78% of the total air pollution with CO in particular is about 97% attributed to mobile sources [28].

RESULTS AND DISCUSSIONS

Numerical data has been analyzed using MATLAB and the graphical representations and analysis given in the sequel. This study has utilized computational fluid dynamics modeling to simulate the transportation of carbon emissions from a 2-lane road environment with embankments of different heights. The simulations have shown the right trend by systematically predicting the concentrations immediately after the source with higher concentration density downward from the source and less concentration density upward from the source. The results from the simulations compare the density of clean air taken as 1.290Kg/m^3 with the density of polluted air in the presence of embankment. Air polluted with gaseous compounds of carbon was expected to have higher density than clean air given that CO has a density of 1.778Kg/m^3.

The graphs in figures 5 below have depicted the distribution of diesel exhaust particles showing the relationship between pollutants concentration density in Kg/m^3 verses the different vertical heights in feet for a(time step=100s), b(time step=200s), c(time step=500s), d(time step=1000s), e(time step=1500s), and f(time step=2000s). From the same graphs it has been clearly seen that the concentration of pollutants spread faster downwards than upwards from the source. For example at time step of 1500seconds the concentration at a vertical height of 10feet was about 1.320Kg/m^{3}while at the same time step at a vertical height of 30feet the concentration was 1.295Kg/m^3. This has been contributed to by the influence of the gravitational source term which

accounts for the gravitational pull on each pollutant. Therefore the upward deflection is affected by gravity on individual particles hence more concentration of the pollutants on the roadway.

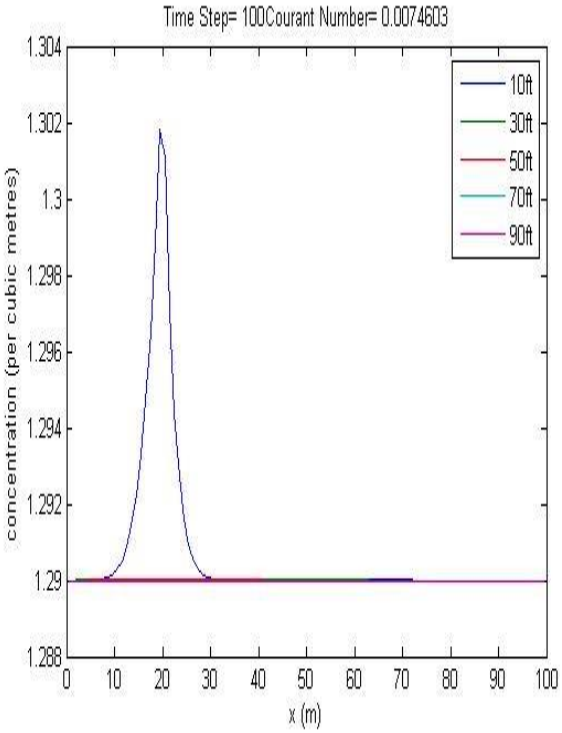

Fig.5 (a)

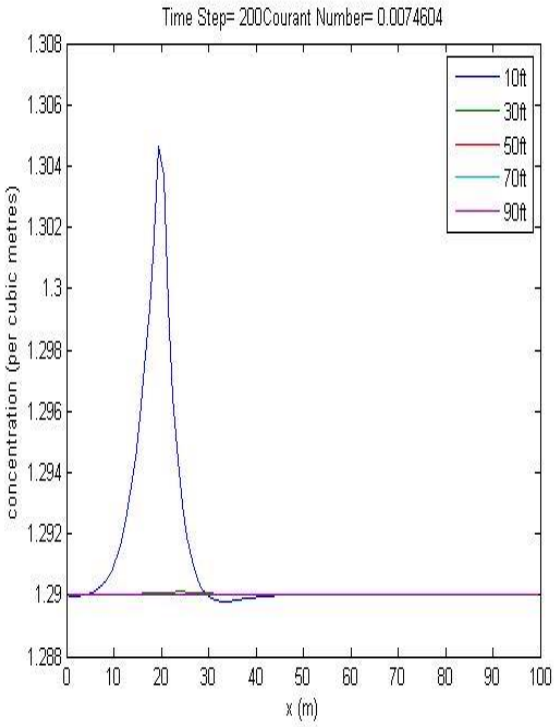

Fig.5 (b)

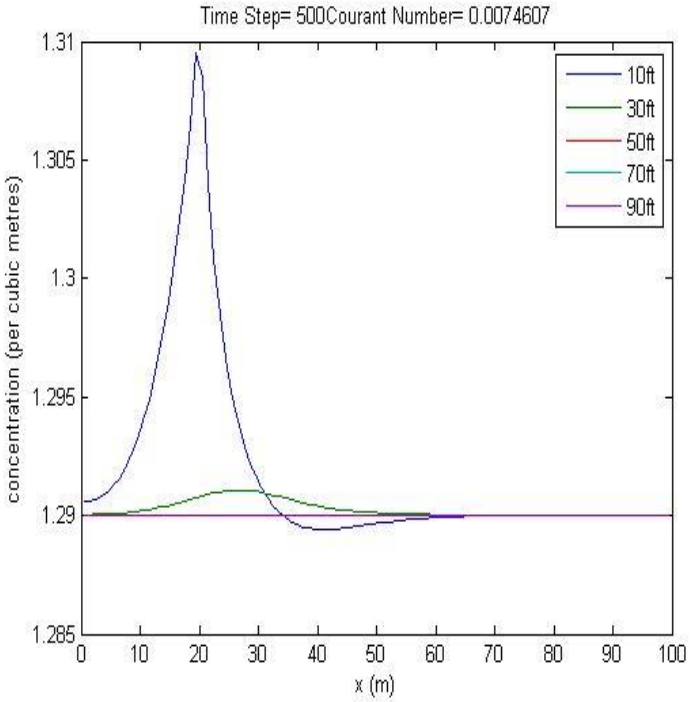

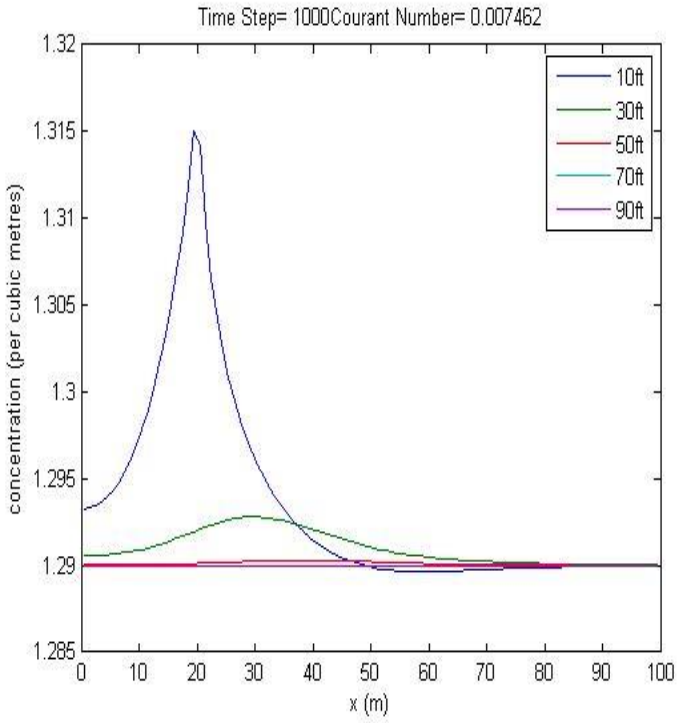

Fig.5(c)

Fig.5 (d)

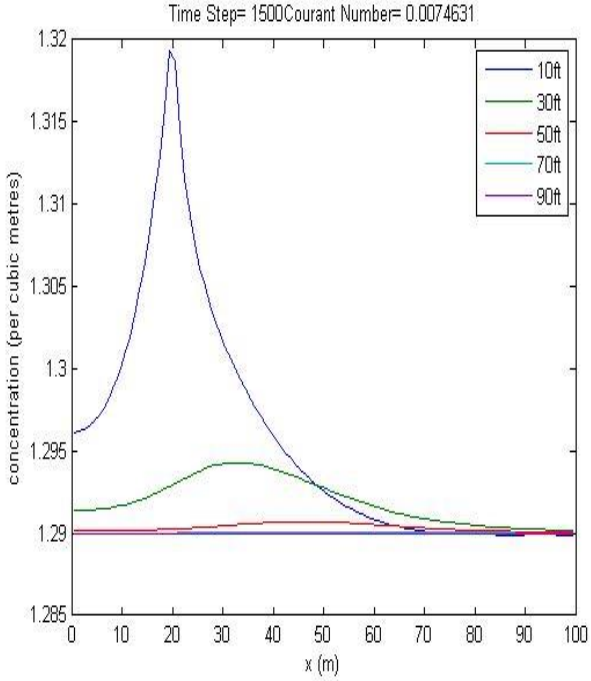

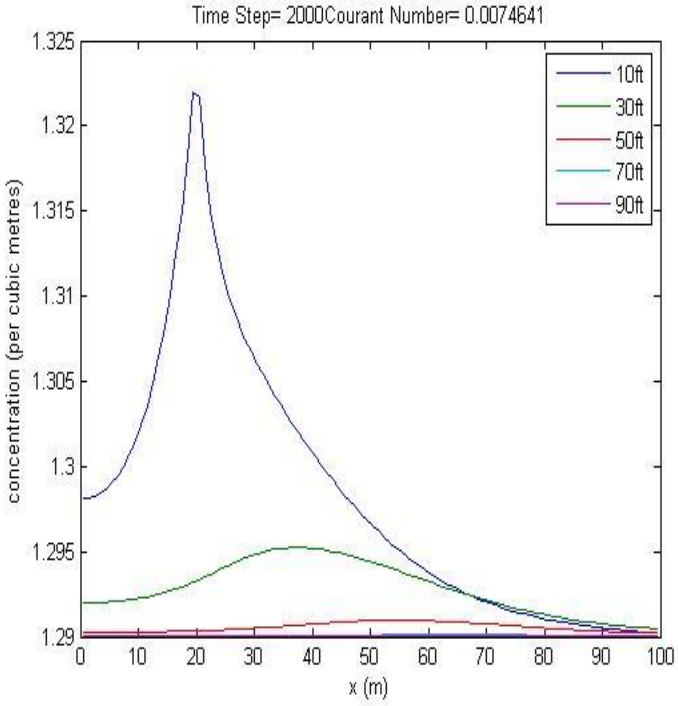

Fig.5 (e)

Fig.5 (f)

The graphs in Fig 6 below have been used to investigate the horizontal on-road concentration profile of pollutants on the cross-road for a(time step=100s), b(time step=200s), c(time step=500s), d(time step=1000s), e(time step=1500s), and f(time step=2000s).. The exhaust has been taken to be at a distant of 20m from the barrier. Comparing the spread of the pollutants at some equal distant from the source say at 10m to the left and right of the source, the concentration was higher at 10m than at 30m.This has been attributed to luck of free flow of the wind as both diffusion and advection are affected by the presence of the embankments. The presence of embankments has also lead to a mixing zone located in the wake of the embankment, where small degree of emissions significantly increased concentrations immediately behind the embankments.

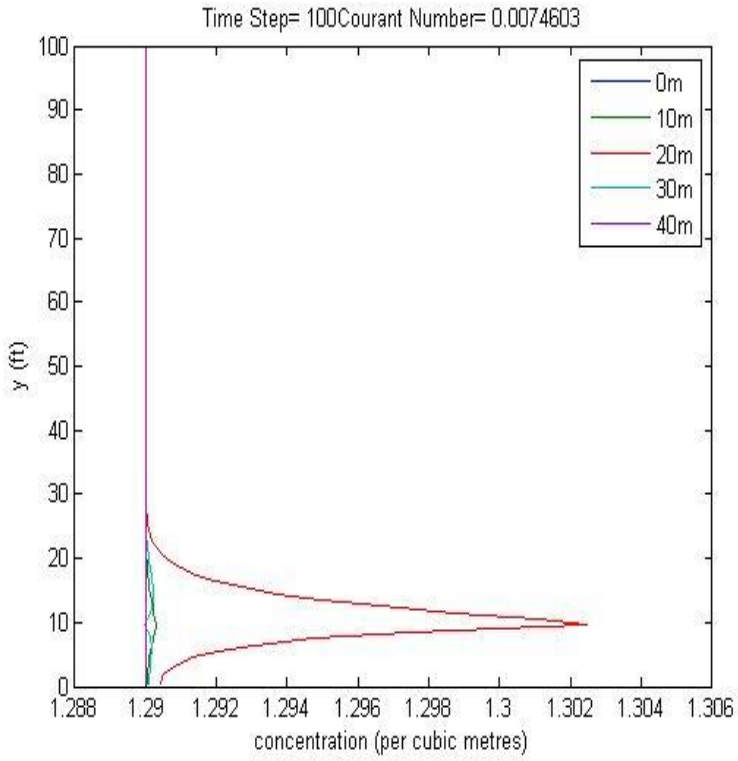

Fig.6(a)

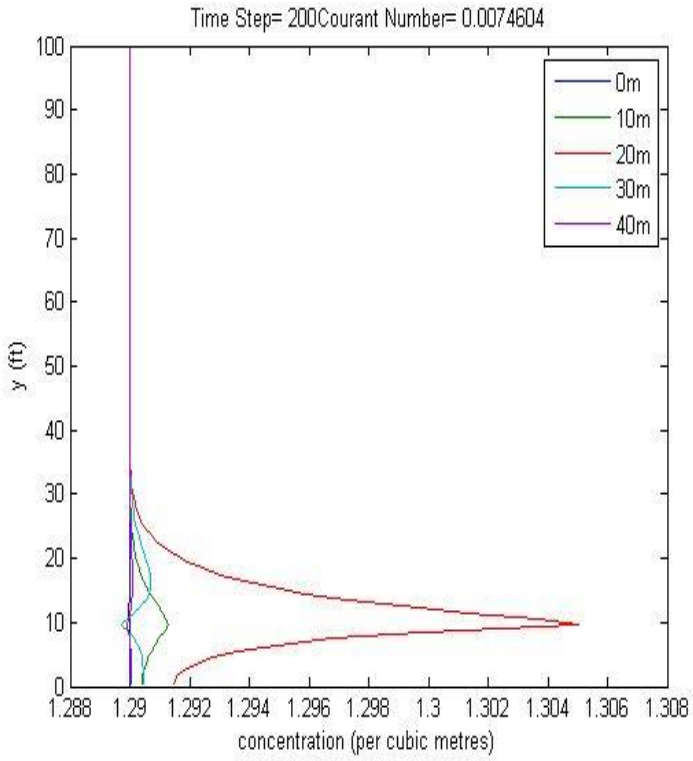

Fig.6(b)

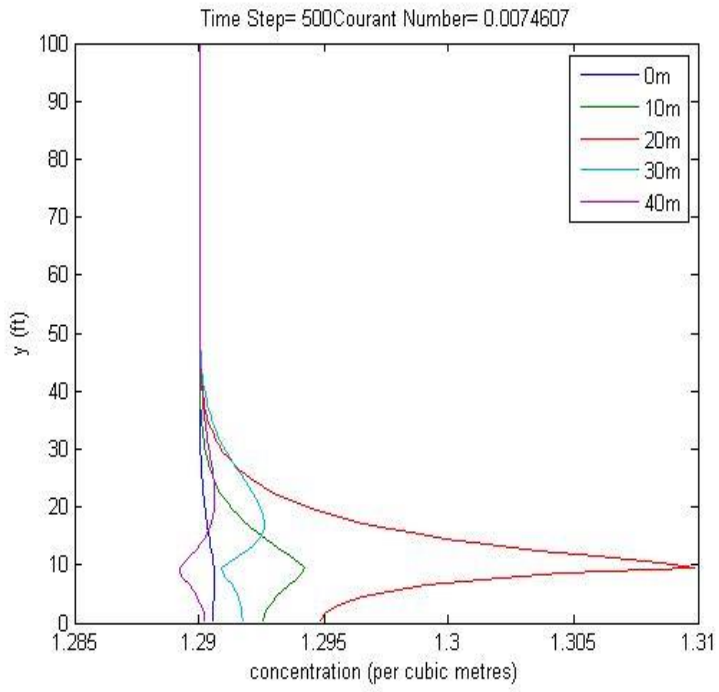

Fig.6(c)

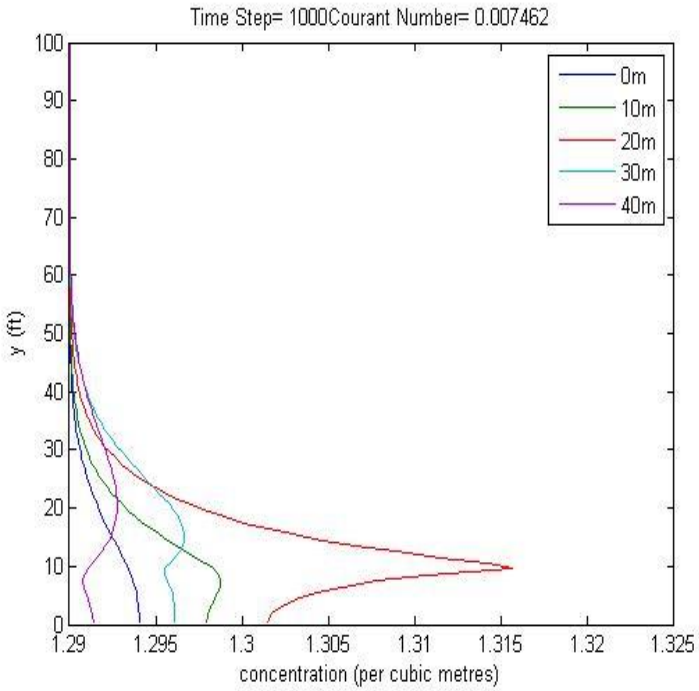

Fig.6(d)

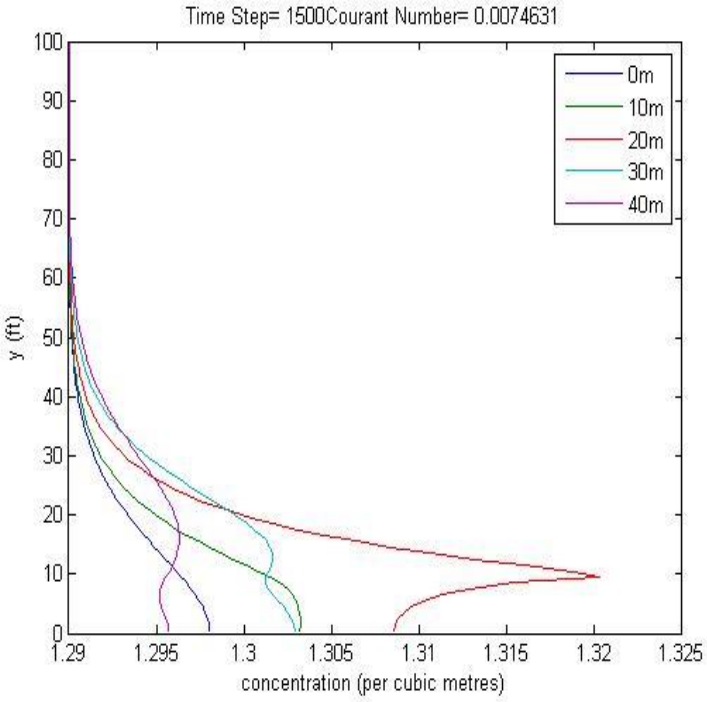

Fig.6 (e)

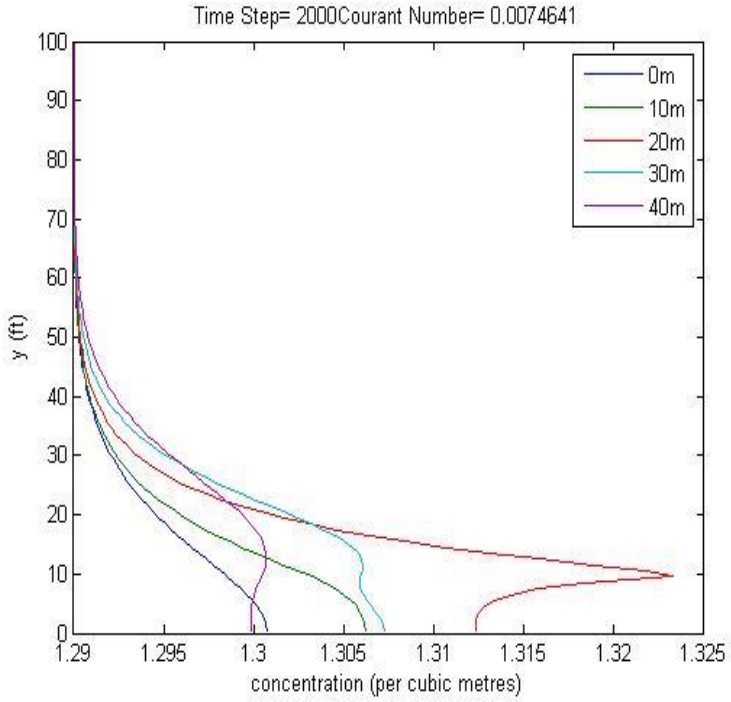

Fig.6 (f)

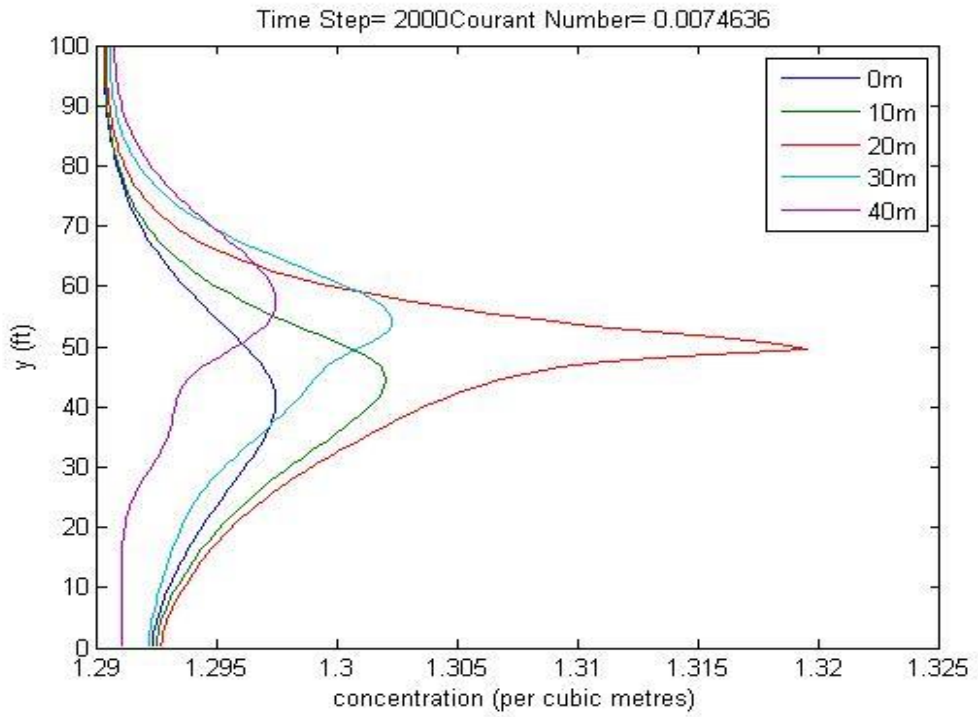

Fig.6 (g)

The level sets in Fig 7 below have given comparison of ground-level simulated concentration of vehicle exhaust for a(time step=100s), b(time step=200s), c(time step=500s), d(time step=1000s), e(time step=1500s), and f(time step=2000s). The simulated results have clearly indicated that the vertical profiles show higher concentrations near the roadway height and lower concentrations vertically higher. Thus it is true that there would be higher concentrations of the pollutants closer to road surface due to embankments which prevent free flow of the wind.

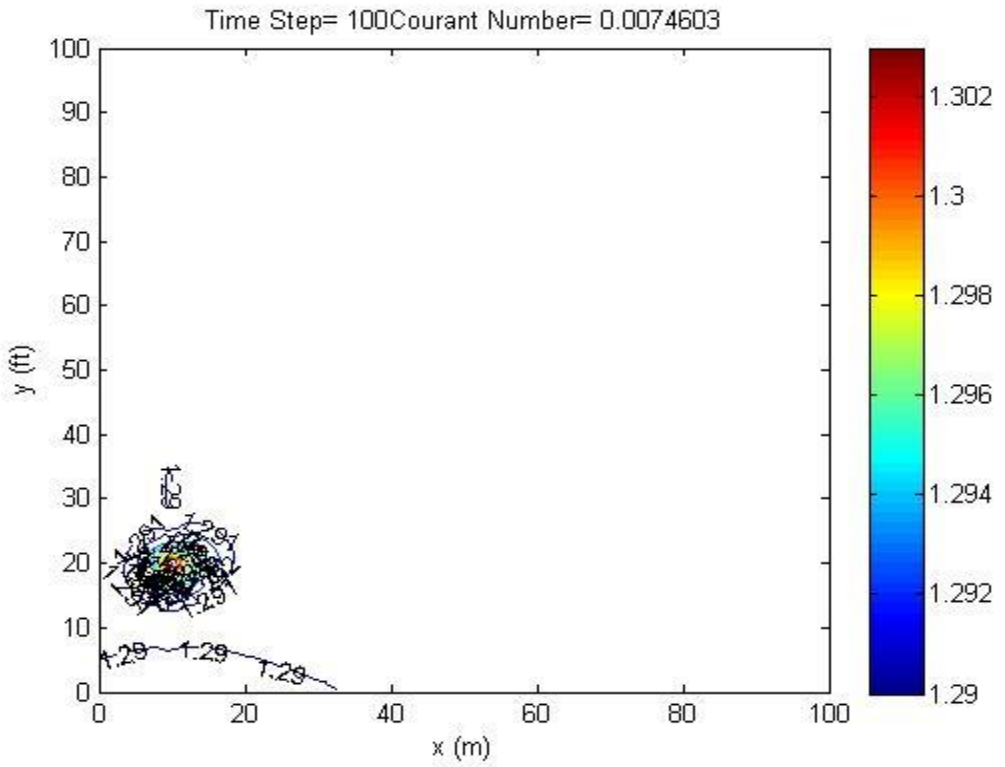
Time Step= 100Courant Number= 0.0074603
y (ft)
x (m)
1.302
1.3
1.298
1.296
1.294
1.292
1.29

Fig.7 (a)

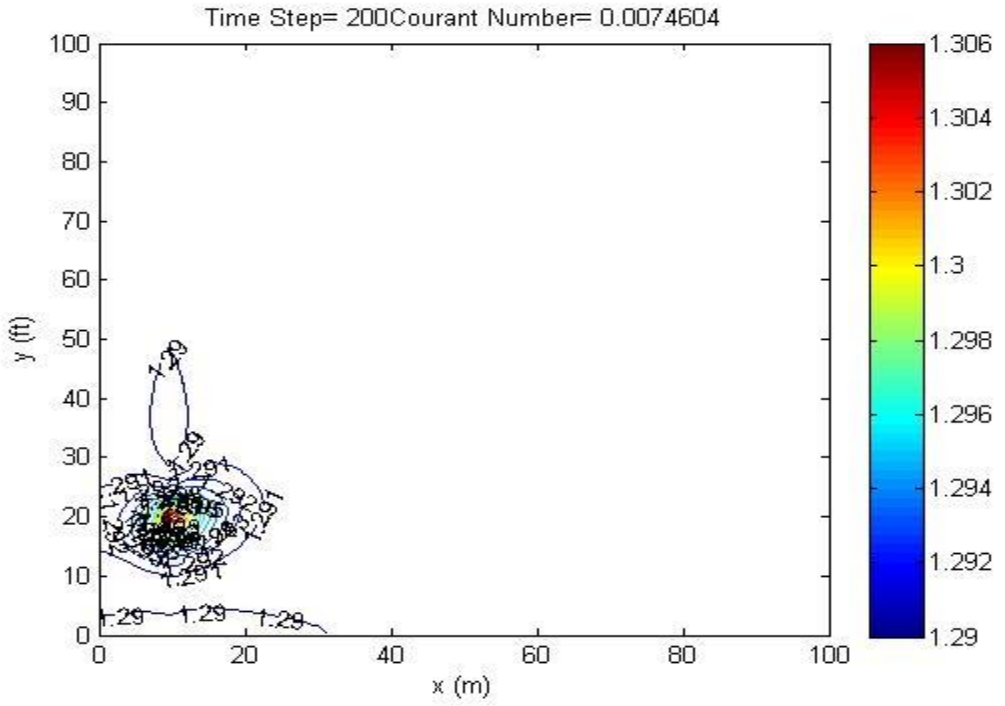
Time Step= 200Courant Number= 0.0074604
y (ft)
x (m)
1.306
1.304
1.302
1.3
1.298
1.296
1.294
1.292
1.29

Fig.7 (b)

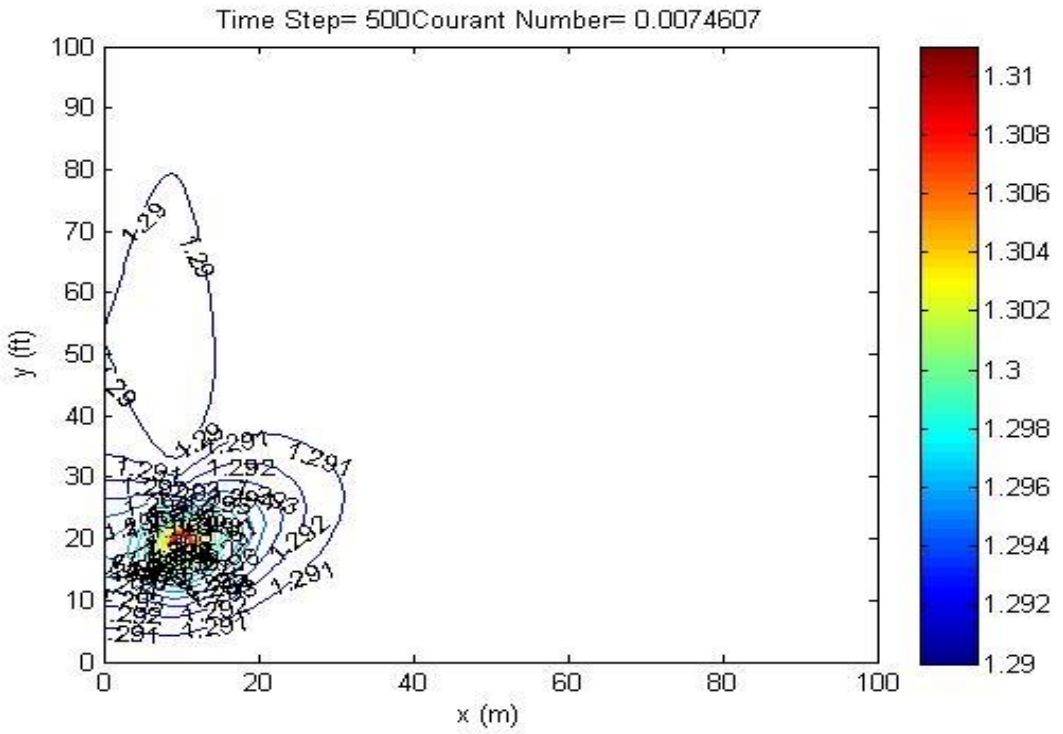
Time Step= 500Courant Number= 0.0074607
y (ft)
x (m)
1.31
1.308
1.306
1.304
1.302
1.3
1.298
1.296
1.294
1.292
1.29

Fig.7(c)

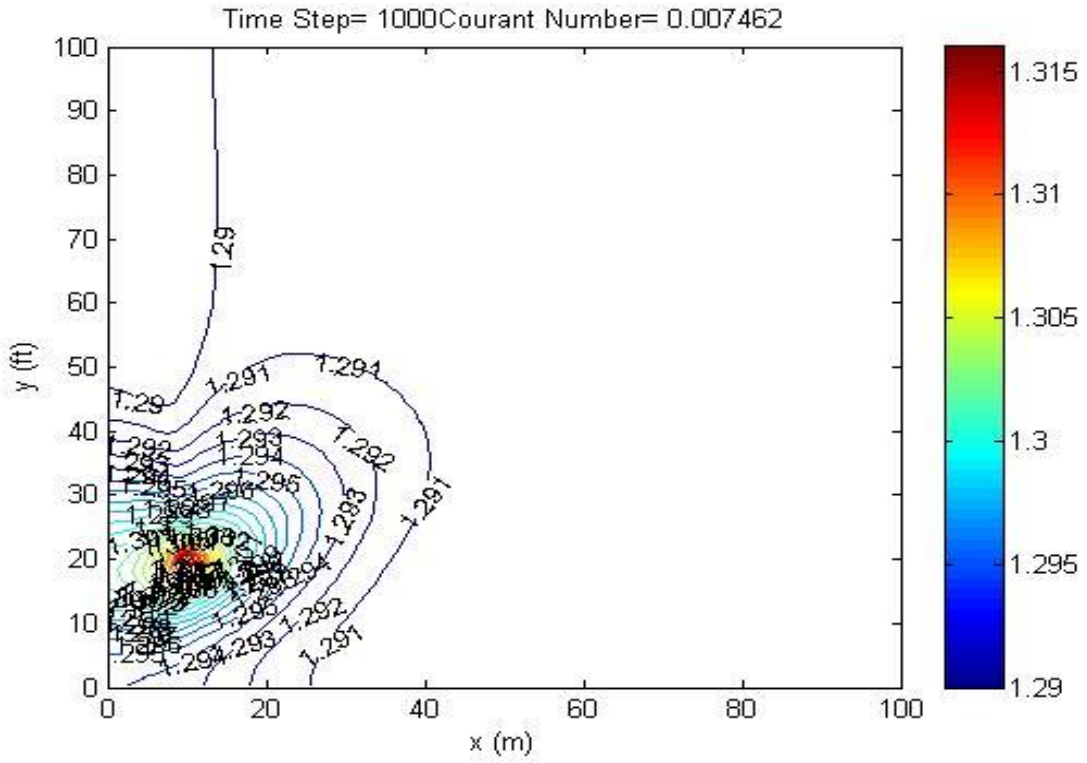
Time Step= 1000Courant Number= 0.007462
y (ft)
x (m)
1.315
1.31
1.305
1.3
1.295
1.29

Fig.7 (d)

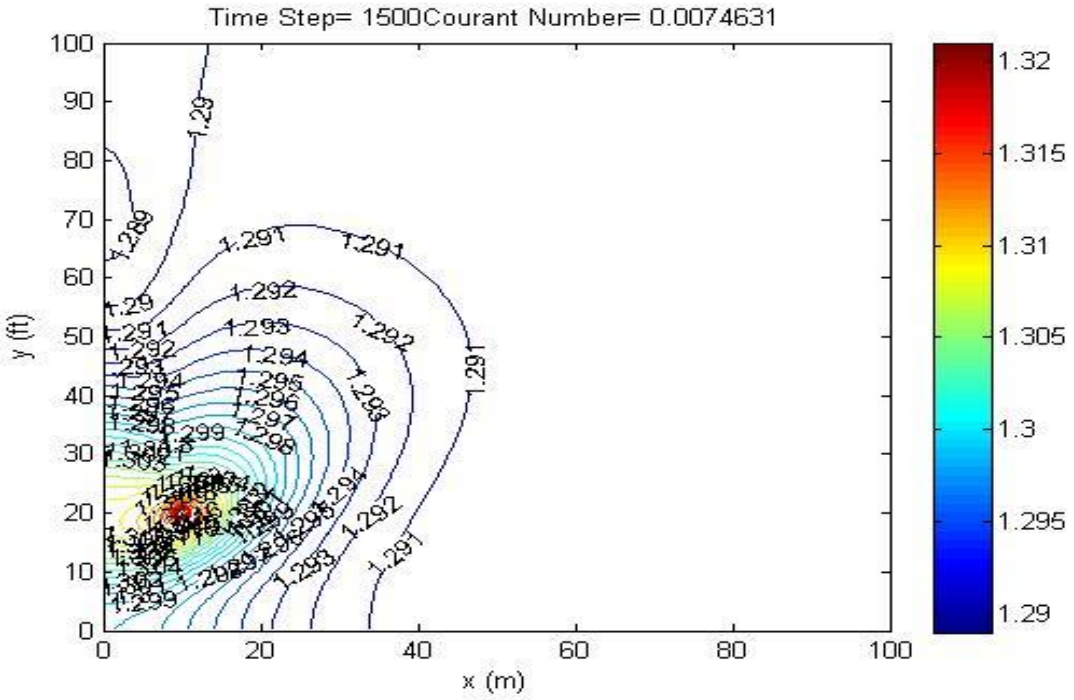
Time Step= 1500Courant Number= 0.0074631
y (ft)
x (m)
1.32
1.315
1.31
1.305
1.3
1.295
1.29

Fig.7 (e)

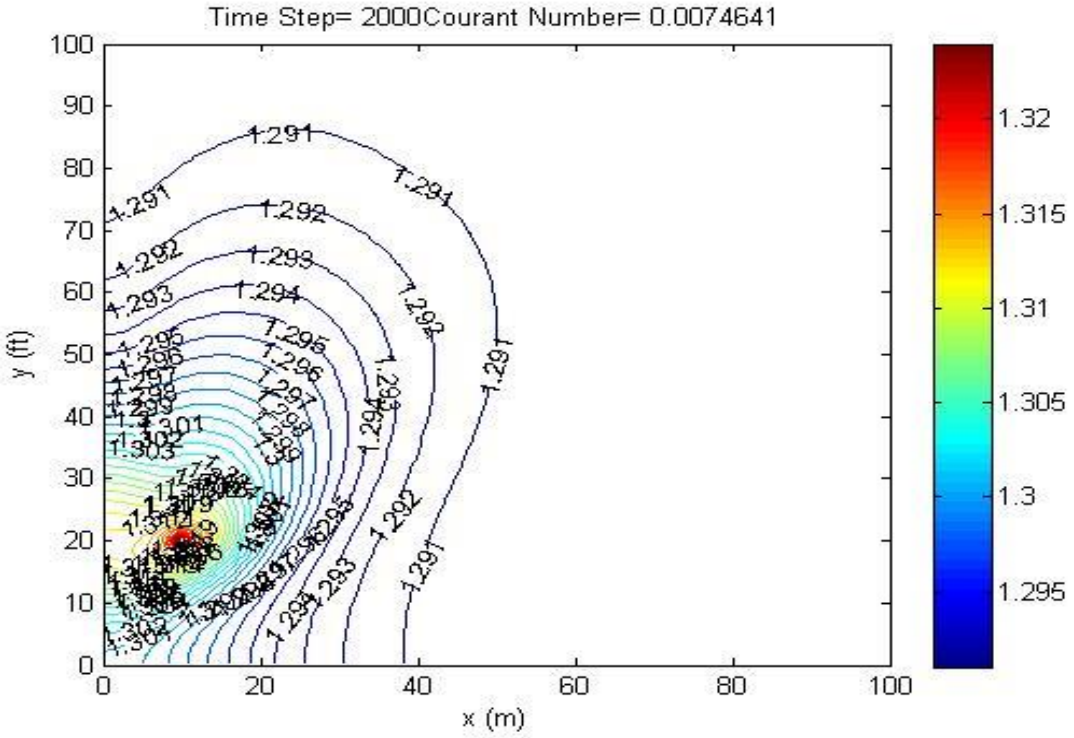
Time Step= 2000Courant Number= 0.0074641
y (ft)
x (m)
1.32
1.315
1.31
1.305
1.3
1.295

Fig.7 (f)

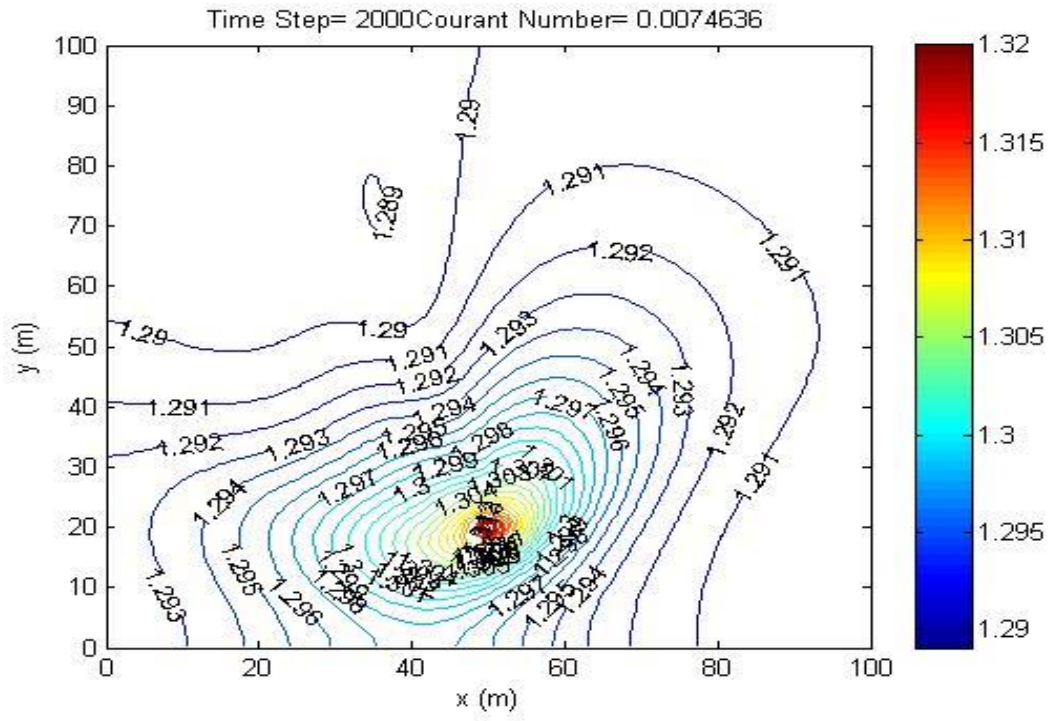

Fig.7 (g)

In all above cases the concentrations of the pollutants have been seen to increase with time, and air becomes free of the pollutants upwards and sideways away from the source. Clearly from the regulatory point of view when no barriers exist, the concentrations of carbon would be relatively low in the road area but instead diffuse outwards in the outer space. The barriers have the bad effect of placing pollution at a higher concentration in the atmosphere closure to the pedestrians with the double barriers worse than a single barrier. As a rule, concentrations of particles decrease as a function of distance from the source due to the various processes as well as dispersion and coagulation.

STABILITY OF THE MODEL

The center manifold theorem by Castillo-Chavez has been considered [18]. Consider the following general system of ordinary differential equations with a parameter U such that:

$\frac{dc}{dt} = f(c, U)$, f: $\mathbb{R}^n \times \mathbb{R}^n \to \mathbb{R}^n$ and $f \in c^2(\mathbb{R}^n \times \mathbb{R}^n)$

Where 0 is the equilibrium point of the system that is $f(0, U) = 0$ for all U and;

$A = \Delta c f(0,0) = \left(\frac{\partial f_i}{\partial c_j}(0,0)\right)$ is the linearization matrix of the system around the equilibrium 0 with Uevaluated at 0.

Zero is simple eigenvalue of **A** and all other eigenvector of **A** have negative real parts.

Matrix **A** has a right eigenvectors $\tilde{K}_R$ and left eigenvector $\tilde{K}_L$corresponding to zero eigenvalues.

Let f_k be the k^{th}component of f and

$$a = \sum_{k_i,j=1}^{n} v_n k_i k_j \frac{\partial^2 u_R}{\partial x_i \partial x_j}(0,0)$$

$$b = \sum_{k_i,j=1}^{n} v_k k_j \frac{\partial^2 u_R}{\partial x_j \partial \alpha}(0,0)$$

The local dynamics of the system around the equilibrium point is totally determined by the signs of a and b particularly, if $a > 0$ and $b > 0$then a backward bifurcation occurs at $U = 0$.

The local dynamics of the system around 0 are totally governed by the sign of a and b.

$a > 0, b > 0,$when $U < 0$ with $|U| << 1,0$ is locally asymptotically stable and there exists a positive unstable equilibrium when $0 < |U| << 1,0$ is unstable and there exists a negative and locally asymptotically stable equilibrium.

$a < 0, b < 0$When$U < 0$ with $|U| << 1,0$ is unstable, when $0 < |U| << 1,0$ is asymptotically stable and there exists a positive unstable equilibrium.

$a > 0, b > 0,$When$U < 0$ with $|U| << 1,0$is unstable and there exists a locally asymptotically stable negative equilibrium, when $0 < |U| << 1,0$ is stable and a positive unstable equilibrium appears.

$a > 0, b > 0,$When U changes from negative to positive, 0 changes its stability from stable to unstable. Corresponding negative unstable equilibrium becomes positive and locally asymptotically stable.

CONCLUSION

Based on the above observations it would be advisable to recommend that the positioning of a car exhaust be located at heights above the car for enhanced diffusion of pollutants into the outer space. Equally important to the road designers, it would be advisable not to construct embankments in towns where traffic jam is a common problem to save pedestrians from inhaling too much carbon that would otherwise endanger their lives.

REFERENCES

[1] **Deyong W., John C. Lin., Dylan B. Millet, Ariel F. Stein, and Roland R. D**.,A backward-time stochastic Lagrangian air quality model,*Department of Soil, Water and Climate, University of Minnesota, USA*,2012.

[2] **Jill Baumgartner**, Journal on Highway proximity and black carbon from cookstove, *McGill University,China*, 2014.

[3] **Ragland and Peirce J. J.,**Boundary Layer Model for Air Pollutant Concentrations Due to Highway Traffic:*University of Wisconsin-Madison*,2012.

[4] **Desmond A., Martin J.,** Evaluation of Model for Air Pollution in the Vicinity of Roadside Barriers. *School of Engineering, Nazarbayev University, Republic of Kazakhstan.School of Engineering, & ICT, University of Tasmania, Australia, 2014.*

[5] **Richard Revesz and Lawrence King,** the wall street jounal on Carbon pollution *New York,U.S.A*, 2014.

[6] **TeimurazD.,**Mathematical Modeling Pollution From Heavy Traffic in Tbilisi Streets:*I.Vekua Institute of Applied Mathematics of Tbilisi State University, Georgia*,2012.

[7] **Alan M.J, Roy M.H.,** Interpretation of Particulate Element and Organic Carbon Concentration at Rural, Urban, and Kerbside Sites.*Division of Environmental Health & Risk Management. The University of Birmingham Edgbaston, Birmingham B15 2TT, United Kingdom, 2004.*
[8] **Yip S.,***Handbook of Materials Modeling; Methods and Models:* Springer, Netherlands,2005.
[9] **Jonathan T. S, Yan J. W, Zhang K. M.,** Exploration of effects of a vegetation barrier on particle size distributions in a near-road environment: *Sibley School of Mechanical and Aerospace Engineering,Cornell University, Ithaca, NY 14853, USA*,2011.

[10] **Jonathan T.S, David K.S, Isakov V, Baldauf R.W, Zhang K.M**, Effects of Roadway Configuration on Near-Road Air Quality and the Implications on Road Designs. *Journal homepage J.T.Steffens et.al, 2014.*
[11] **Akul V.,** The Impact of Roadside Barrier on Near-Road Concentration of Traffic Related Pollutants. *Nico Schutle(nschn003@ucr.edu) university of California,USA,2013.*
[12] **Alkalaj.J, Throstuv.**Effect of Vegetation Barriers on Traffic-Related Particulate Matter.*Thorsteinson University of Iceland, Iceland, 2012.*
[13] **Micah Fuller FabiánBombardelli,** Particulate Matter Modeling in Near-Road Vegetation Environments: *Department of civil & environmental engineering university of California, USA*,2009.
[14] **Kahn.R, Kobayashi.S, Bentle M, GascaJ,Lee D.S, Muromachi Y, Newton P.J, Plotkin.S, Sarling. D, Wit. R, Zhon. P.J**,Transport and its Infrustracture. *Cambridge University Press, Cambridge, United Kingdom and New York, NY, USA, 2007.*
[15] **Hoeven.M.V**, CO_2 Emission from Fuel Combustion.*Internation Energy Agency © OECD/IEA Paris Cedex,France, 2014.*
[16] **Satoshi H., Charles N. K., David J.; Nowak,** Development of a distributed air pollutant dry deposition modeling framework:*The Davey Institute, United States*,2012.
[17] **Baldauf. R, Thoma. E, Khystov. A, Isakov. V, Bowker. G, Long. T, Snow. R**. Impact of Noise Barier on Near-Road Air Quality. *Journal Homepage Atmospheric Environment, 2008.*
[18] **Gayle S.W.H, Wei T., Matthew J.F, David K.H,** Model Evaluation of Roadside Barrier Impact on Near-road Air Pollution. *Journal Homepage, US EPA, Office of Research and Development, National Risk Management Research Laboratory, Research Triangle Park, NC27711, USA, 2010.*
[19] **Roorda-Knapeet a l**,BioMed Central Journal Gateways:*Netherlands*,2007.
[20] **Bauver Wesley P.,** Mathematical Modeling Of The Dispersion Of Air Pollutants From Highways, *Wind Energy Center Masters Theses Collection USA*,1978.
[21] **Turner, B.P.,** 'Wookbook of Atrrtospheric Dispersion Estimates,' *Environmental Protection Agency, Office of Air Programs, Research Triangle Park, North Carolina*,1970.
[22] **Hadipour M., Pourebrahim S. and Mahmmud A. R**., Mathematical modeling considering air pollution of transportation: *An urban environmental planning, case study in petalingjaya, malaysia*,2009.
[23] **Michael Hogan,** Roadway Air Dispersion Modeling Theoretical Basis for Atmospheric Diffusion from a Linear Source:*Environmental Systems Laboratory Publishers*,1947.
[24] **Richard J Venti,** Atmospheric diffusion models for roadway source:*ESLInc* 1970.

[25] **Goyal P. And Anikender Kumar,** Mathematical Model of Air Pollutants:*An Application to Indian Urban City, Centre for Atmospheric Sciences Indian Institute of Technology Delhi India*, 2008.
[26] **Murdock, James,** Normal Forms and Unfoldings for Local Dynamical Systems: *Sringers-Verlag*, 2003.
[27] **Odeyo.D.A.,** An Energy Approach to Evaluation of Carbon Dioxide Emission from Kenyan's Road Freight Transport.*Developing Country Studies.Vol 5 No 4, 2015.*
[28] **Olegario. G.V, Rene. V.R.,**Emperical Analysis on the Relationship between Air Pollution and Traffic Flow Parameters. *Teodoro University of the PhillippinesDiliman, Quezon City Proceedings of the Eastern Asia Society for Transportation Studies Vol.1, Autum, 1997.*